Performance Analysis of Opportunistic Scheduling in Dual-Hop Multiuser Underlay Cognitive Network in the Presence of Cochannel Interference

Jamal Ahmed Hussein, *Student Member, IEEE*, Salama S. Ikki, *Member, IEEE*, Said Boussakta, *Senior Member, IEEE*, and Charalampos C. Tsimenidis, *Senior Member, IEEE*

***Abstract*—In this paper, the performance of a dual-hop multiuser underlay cognitive network is thoroughly investigated by using a decode-and-forward (DF) protocol at the relay node and employing opportunistic scheduling at the destination users. A practical scenario where cochannel interference signals are present in the system is considered for the investigation. Considering that transmissions are performed over nonidentical Rayleigh fading channels, first, the exact signal-to-interference-plus-noise ratio (SINR) of the network is formulated. Then, the exact equivalent cumulative distribution function (cdf) and the outage probability of the system SINR are derived. An efficient tight approximation is proposed for the per-hop cdfs, and based on this, the closed-form expressions for the error probability and the ergodic capacity are derived. Furthermore, an asymptotic expression for the cdf of the instantaneous SINR is derived, and a simple and general asymptotic expression for the error probability is presented and discussed. Moreover, adaptive power allocation under the total-transmit-power constraint is studied to minimize the asymptotic average error probability. As expected, the results show that optimum power allocation improves the system performance compared with uniform power allocation. Finally, the theoretical analysis is validated by presenting various numerical results and Monte Carlo simulations.**

***Index Terms*—Cochannel interference (CCI), dual-hop decode-and-forward (DF), ergodic capacity, error probability, optimization, outage probability, underlay cognitive radio (CR).**

I. Introduction

Cognitive radio (CR) has become a more attractive research field in wireless communication for many researchers over the past few years [1]–[5]. This is because of its promise of using the existing frequency spectrum more efficiently. Recently, three paradigms have been proposed for realizing the CR network [2]. Based on the simplicity of implementation, they are underlay, interweave, and overlay. In an underlay CR scheme, there is a strict power constraint on the transmission power [2] for the purpose of the protection of the quality of service (QoS) of the primary user. One of the advantages of using cooperative communication is that the transmitting nodes can broadcast their signals at relatively lower power. This could help an underlay CR scheme in improving its performance. Over the last decade, cooperative communication for different network scenarios has been extensively studied (see, e.g., [6]–[9]).

In [10]–[18], it has been shown that applying an opportunistic selection technique in a cooperative communication network has the advantage of enhancing the performance of the system. Furthermore, in [19], an investigation was done for the performance of the uplink cognitive cellular networks using the opportunistic scheduling of the secondary user, which causes the minimum interference to the primary user. Li in [20] analyzed the effect of maximum ratio combining (MRC) on the single-user CR network. In this paper, the asymptotic formulas for the average error probability and the system ergodic capacity have been obtained.

In [21], the outage probability of the dual-hop single-user amplify-and-forward (AF) cognitive cooperative network was studied by considering a single primary user and over Nakagami-m fading channels. In [22], the performance of the multihop decode-and-forward (DF) underlay single-user CR network was investigated over Rayleigh fading channels. The asymptotic outage probability of the dual-hop AF CR network was derived in [23] under the assumption that the primary transmitter causes interference to the secondary network. Furthermore, Huang *et al.* in [24] studied the outage performance of the multiuser dual-hop DF underlay CR over Nakagami-m fading channels in the presence of the primary transmitter. In their calculations, signal-to-noise ratio (SNR)-based and signal-to-interference-plus-noise ratio (SINR)-based scheduling algorithms have been used to derive the outage performance formula.

Bao *et al.* in [25] investigated the outage probability of the multirelay spectrum-sharing network. The best relay selection technique was employed, such that it enhances the overall performance of the network. In their analysis, the power limit constraint on the secondary transmit nodes was not considered. The outage and error probability of a multiple-input multiple-output (MIMO) underlay CR network was investigated in [26]. To improve the performance of the secondary network, the

Manuscript received January 29, 2015; revised September 10, 2015; accepted October 28, 2015. Date of publication November 26, 2015; date of current version October 13, 2016. This work was supported in part by Leverhulme Trust under Grant VP1-2012-008, by the Engineering and Physical Sciences Research Council under Grant EP/11004637/1, and by The Higher Committee for Education Development in Iraq. The review of this paper was coordinated by Prof. C. Lin.

J. A. Hussein, S. Boussakta, and C. C. Tsimenidis are with the School of Electrical and Electronic Engineering, Newcastle University, Newcastle Upon Tyne NE1 7RU, U.K. (e-mail: j.hussein@ncl.ac.uk; said.boussakta@ncl.ac.uk; charalampos.tsimenidis@ncl.ac.uk).

S. S. Ikki is with the Department of Electrical Engineering, Lakehead University, Thunder Bay, ON P7B 5E1, Canada (e-mail: sikki@lakeheadu.ca).

Color versions of one or more of the figures in this paper are available online at http://ieeexplore.ieee.org.

Digital Object Identifier 10.1109/TVT.2015.2504244

MRC technique was used at the secondary receiver nodes. The throughput analysis of the dual-hop DF multiantenna CR network was investigated in [27]. Moreover, in [28], transmit antenna selection with the MRC technique was used to evaluate the outage probability of the dual-hop DF MIMO underlay cognitive networks. The impact of the primary transmitter and the imperfect channel state information were considered in their calculation.

The outage probability, average error probability, and ergodic capacity performance was investigated in [29]. A single destination user node was considered, and interferences on the secondary network were not considered. The outage performance of the multiuser spectrum-sharing network was investigated in [30]. In their analysis, the selection-combining method was used to improve the performance of the secondary network. In [31], the outage probability, average outage duration, and average outage rate for the multirelay underlay CR network were studied by using the best relay selection method. In [32], the outage performance of the dual-hop DF CR was investigated in the presence of a single node at each of the source, relay, and destination. Finally, the opportunistic scheduling technique was used to enhance the outage performance of the multisource underlay CR network [33].

In most of the previous studies in the area of underlay CR networks, the outage performance has been extensively studied for different system models. In addition, few works have investigated the error probability and/or capacity performance. However, the impact of the cochannel interference (CCI) on the multiuser underlay CR network has not been studied. Furthermore, a detailed investigation of the error probability and the capacity performance for the opportunistic multiuser cooperative CR has not been previously carried out. Moreover, the adaptive power allocation under the total-transmit-power constraint and the impact of CCI have not been studied.

Consideration of CCI is indeed necessary because of the aggressive reuse of frequency channels for high spectrum utilization in different wireless systems, and multiuser dual-hop underlay CR networks are no exception. Due to the broadcast nature of wireless signal transmissions, interference always exists over a wide range of frequency bands in almost all practical wireless communication systems. For example, interference may come from other authorized users of the same spectrum or from other frequency channels injecting energy into the channel of interest [34].

This paper provides a comprehensive performance analysis for the effect of CCI in practical multiuser dual-hop underlay CR networks, considering independent nonidentical Rayleigh fading channels affecting the relay and destination nodes, specifically using the DF scheme at the relay node and applying the opportunistic scheduling technique at the destination. The outage probability, error probability, and ergodic capacity are investigated assuming that a finite number of CCI signal affects each relay as well as the destination nodes.

The remainder of this paper is organized as follows: The following section is for presenting the system model and its mathematical representation. In Section III, the derivations of the performance metrics are presented. Simulated and analytical results for the evaluation and proof of the derived expressions are provided in Section IV. Section V presents the summary and conclusions of this work. Finally, we give detailed steps of the analytical derivations in Appendices A–D.

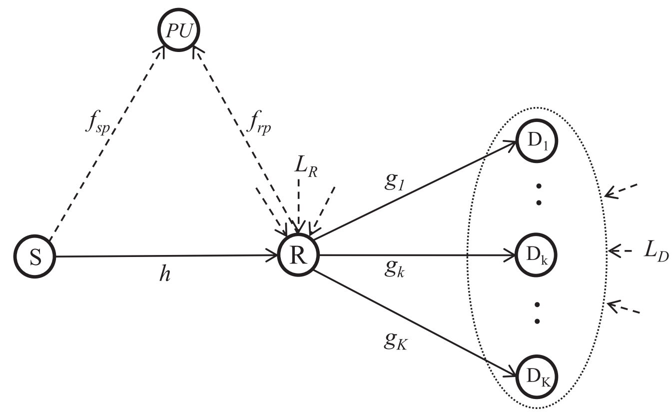

Fig. 1. General system model used for analysis.

II. System Model

As shown in Fig. 1, we consider a cognitive network of one source node (S), one relay node (R), K destination users $(D_k, k = 1, 2, \ldots, K)$, and a single primary-user node. The nodes in the system are equipped with a single antenna and operate in half-duplex mode. In our system model, we assume that the impact of the primary transmitter on the secondary network in this specific cell is neglected. One of the possible examples of our system model is when the same network provider controls both primary and secondary nodes, where the level of interference with the secondary users can be controlled within a reasonable range. This can be obtained by managing the nodes according to their position, or it could be possible to interpret the interference as a further addition to the existing noise level at the secondary-user receiver [29]. Moreover, the impact of other transmit nodes in the neighboring cells cannot be ignored. We have expressed the interference from outside our cell as the CCI to our network. Another possible example of our system model is to represent the impact of the primary transmitter and the other surrounding transmit nodes as the CCI. This is due to the fact that the CCI could be from any other frequency channels injecting energy into the channel of interest.

In addition, we assume that there is no direct link between the secondary source and destination nodes [24] (i.e., the communication is performed through the relay node only). Moreover, we define $I_{\max}$ as a threshold interference value, which is the maximum tolerance of interference that the secondary transmit nodes can produce at primary receiver nodes [34], [35]. The channels in the dual-hop communication are assumed to be affected by independent nonidentical slow Rayleigh fading channels. In addition, we assume that the destination nodes are distributed in a homogeneous environment; therefore, the channels between the relay node and K destination users are affected by the independent and identically distributed Rayleigh fading channels [10], [12], where h and g_k are the channel coefficients between source–relay and relay–kth destination, respectively, and f_{sp} and f_{rp} are the interference channel coefficients between secondary source–primary receiver and secondary relay–primary receiver, respectively. Therefore, the corresponding channel gains will be $|h|^2$, $|g_k|^2$, $|f_{sp}|^2$, and $|f_{rp}|^2$ that follow an exponential distribution with mean values of σ_h^2, σ_g^2, $\sigma_{f_{sp}}^2$, and $\sigma_{f_{rp}}^2$, respectively. In our system model, we consider the transmission power constraint on the secondary transmit nodes. For example, P_s represents the maximum power that the secondary source can achieve. Similarly, P_r is the maximum power that the secondary relay can use.

In the DF relay protocol, transmission is performed within two phases (i.e., time slots). In the first phase of transmission, the source node will transmit the signal to the relay node using its permitted power. The received signal at the relay node has the following form:

$$y_r = \sqrt{E_{us}}hx + \sqrt{E_{IR}}\sum_{j=1}^{L_R} q_j x_j + n_r \tag{1}$$

where E_{us} is the actual transmit power at the source node (i.e., permitted transmission power), i.e., $E_{us} = \min((I_{\max}/|f_{sp}|^2), P_s)$. x is the transmitted signal with unit energy. E_{IR} is the interference power at the relay node, q_j is the fading channel coefficient between the jth interferer and the relay, x_j is the jth interferer signal, and n_r is the additive white Gaussian noise (AWGN) at the relay node that has a power spectral density (PSD) of N_0. Furthermore, L_R is the total number of interferers that affect the relay node.

In the second phase of transmission, the relay node will decode the received message from the source node, and then, it will encode it and forward it to the destination users. The received signal at each of the destination users has the following form:

$$y_{D_k} = \sqrt{E_{ur}}g_k\hat{x} + \sqrt{E_{ID_k}}\sum_{i=1}^{L_D} p_{ki}x_{ki} + n_{d_k} \tag{2}$$

where E_{ur} is the actual transmit power at the relay node, i.e., $E_{ur} = \min((I_{\max}/|f_{rp}|^2), P_r)$. $\hat{x}$ is the transmitted signal from the relay node. E_{ID_k} is the interference power at the kth user, p_{ki} is the fading channel coefficient between the ith interferer and the kth user, x_{ki} is the ith interferer signal, and n_{d_k} represents the AWGN at the kth destination user that has a PSD of N_0. Furthermore, L_D denotes the total number of interferers that affect the destination nodes.

Thus, the instantaneous SINR at the input of the relay and the kth destination node can be, respectively, expressed as

$$\gamma_h^{\text{eff}} = \frac{\gamma_h}{1 + \sum_{j=1}^{L_R} I_{Rj}} \tag{3}$$

$$\gamma_{g_k}^{\text{eff}} = \frac{\gamma_{g_k}}{1 + \sum_{i=1}^{L_D} I_{D_{ki}}}, \quad k = 1, 2, \ldots, K \tag{4}$$

where $\gamma_h = \min((I_{\max}/|f_{sp}|^2), P_s)|h|^2/N_0$ and $\gamma_{g_k} = \min((I_{\max}/|f_{rp}|^2), P_r)|g_k|^2/N_0$ are the instantaneous SNR at the relay and the kth destination nodes, respectively, and I_{Rj}, $(j = 1, 2, \ldots, L_R)$ and I_{Di}, $(i = 1, 2, \ldots, L_D)$ are the instantaneous interference-to-noise ratio (INR) at the relay and any destination nodes, respectively. The instantaneous INRs I_{Rj} and I_{Di} are random variables (RVs) that follow the exponential distribution with mean values of $\bar{I}_R$ and $\bar{I}_D$, respectively.

In our system model, we assume that the CCI sources are far enough from the relay and destination nodes such that, although the CCI sources are randomly distributed geographically, the distance from the interferers to the relay and the destination nodes can be assumed to be the same. Therefore, it can be assumed that the received interference signals at the relay and destination nodes are identical in terms of the average energy [12], [36]. This example can be observed in a conventional cellular network with deterministic number of nodes, in which it is reasonable to assume that all the nodes will receive interference from an equal number of nodes [12], [37]. It is worth mentioning that our derivations in this work are based on average values rather than instantaneous values.

Opportunistic scheduling is achieved by selecting the destination with the highest instantaneous SINR out of K destinations, at any particular point in time. The highest instantaneous SINR of the selected user (i.e., strongest user), which is denoted as $\gamma_{\text{eq}}^{\text{opp}}$, is determined by [38], [39]

$$\gamma_{\text{eq}}^{\text{opp}} = \min\left(\gamma_h^{\text{eff}}, \gamma_{g*}\right) \tag{5}$$

where

$$\gamma_{g*} = \min\left(\frac{I_{\max}}{N_0|f_{rp}|^2}, \frac{P_r}{N_0}\right) \max_{k=1,\ldots,K}\left\{\frac{|g_k|^2}{1+\sum_{i=1}^{L_D} I_{D_{ki}}}\right\}. \tag{6}$$

III. Performance Evaluation

A. CDF of $\gamma_{\text{eq}}^{\text{opp}}$

In a dual-hop cooperative communication, the cumulative distribution function (cdf) of the end-to-end opportunistic SINR named as $F_{\gamma_{\text{eq}}^{\text{opp}}}(\gamma)$ can be expressed as [9]

$$F_{\gamma_{\text{eq}}^{\text{opp}}}(\gamma) = 1 - \left(1 - F_{\gamma_h^{\text{eff}}}(\gamma)\right)\left(1 - F_{\gamma_{g*}}(\gamma)\right) \tag{7}$$

where $F_{\gamma_{g*}}(\gamma)$ is the cdf of the SINR received at the terminal of the selected user. $F_{\gamma_h^{\text{eff}}}(\gamma)$ and $F_{\gamma_{g*}}(\gamma)$ are the cdfs of γ_h^{eff} and γ_{g*}, respectively. The cdfs of γ_h^{eff} and γ_{g*} can be found as follows.

1) Determining $F_{\gamma_h^{\text{eff}}}(\gamma)$: The first-hop cdf is derived as follows.

Corollary 1: The equivalent cdf of the first-hop SINR can be written as in (8), shown at the bottom of the next page.

Proof: See Appendix A.

2) Determining $F_{\gamma_{g*}}(\gamma)$: Using quite similar steps, the cdf of γ_{g*} can be written as in (9), shown at the bottom of the next page. For this part, we use different notations corresponding to the second-hop entities, such that we replace σ_h^2, $\sigma_{f_{sp}}^2$, L_R, and $\bar{I}_R$ with σ_g^2, $\sigma_{f_{rp}}^2$, L_D, and $\bar{I}_D$, respectively.

Bearing in mind that the cdf of the maximum SINR out of K users (i.e., $\max_{k=1,\ldots,K}\{|g_k|^2/(1+\sum_{i=1}^{L_D} I_{D_{ki}})\}$) can be expressed as $F_{\max_{k=1,\ldots,K}\{|g_k|^2/(1+\sum_{i=1}^{L_D} I_{D_{ki}})\}}(\gamma) = [1 - e^{-(\gamma/\sigma_g^2)}(\sigma_g^2/(\sigma_g^2+\gamma\bar{I}_D))^{L_D}]^K$.

By substituting the derived cdf expressions $F_{\gamma_h^{\text{eff}}}(\gamma)$ and $F_{\gamma_{g*}}(\gamma)$ in (8) and (9), respectively, into (7), an exact cdf expression of $\gamma_{\text{eq}}^{\text{opp}}$ can be obtained.

The equivalent opportunistic outage probability is defined as the probability that the equivalent SINR is below a predefined threshold value; this can be easily obtained from the previous calculated equivalent cdf by replacing variable γ with $\gamma_{\rm th}$, i.e.,

$$P_{\rm out}^{\rm opp}(\gamma_{\rm th}) = \Pr\left(\gamma_{\rm eq}^{\rm opp} \leq \gamma_{\rm th}\right) = F_{\gamma_{\rm eq}^{\rm opp}}(\gamma_{\rm th}). \tag{10}$$

B. Average Error Probability

The average error probability performance can be investigated via different approaches. For example, the cdf or the probability density function (pdf) can be used to investigate this performance indicator. By observing the derived per-hop cdfs, it can be deduced that using the cdf approach for this investigation could be more mathematically convenient. Thus, the expression for the average error probability can be obtained using the following formula [37]:

$$\bar{P}_b(e) = \frac{a}{2}\sqrt{\frac{b}{\pi}} \int_0^\infty \frac{\exp(-bx)}{\sqrt{x}} F_{\gamma_{\rm eq}}(x)dx \tag{11}$$

where a and b are arbitrary constants, depending on the modulation schemes (e.g., quaternary phase-shift keying: $a = 2$ and $b = 0.5$) [34]. The average error probability for the first hop and the second hop, i.e., $\bar{P}_b^{sr}(e)$ and $\bar{P}_b^{rd}(e)$, can be obtained by substituting the derived corresponding cdfs (i.e., $F_{\gamma_h^{\rm eff}}(z)$ and $F_{\gamma_{g*}}(z)$) into (11). Finally, the end-to-end average error probability can be calculated using the following equation [40]:

$$\bar{P}_b^{e2e}(e) = \bar{P}_b^{sr}(e) + \bar{P}_b^{rd}(e) - 2\left(\bar{P}_b^{sr}(e)\bar{P}_b^{rd}(e)\right). \tag{12}$$

To calculate the per-hop error probability, we propose the following theorem.

Theorem 1: We are aiming to represent the per-hop equivalent cdfs for both the first and second hops in a simpler form, which is more mathematically convenient, such that we can carry out further investigation of the system performance. First, we employ the following notations for both hops to make the formulas more mathematically tractable.

First-hop cdf notations:

$$\Upsilon_1 = \left(1 - e^{-\frac{I_{\max}}{P_s\sigma_{f_{sp}}^2}}\right)\left(\frac{P_s\sigma_h^2}{\bar{I}_R}\right)^{L_R} \tag{13a}$$

$$\Upsilon_2 = \left(\frac{I_{\max}\sigma_h^2}{\sigma_{f_{sp}}^2}\right)\left(\frac{P_s\sigma_h^2}{\bar{I}_R}\right)^{L_R} e^{-\frac{I_{\max}}{P_s\sigma_{f_{sp}}^2}} \tag{13b}$$

$$\alpha = P_s\sigma_h^2 \tag{13c}$$

$$\beta = \frac{P_s\sigma_h^2}{\bar{I}_R}. \tag{13d}$$

Second-hop opportunistic cdf notations:

$$\Upsilon_3 = \left(1 - e^{-\frac{I_{\max}}{P_r\sigma_{f_{rp}}^2}}\right)\left(\frac{P_r\sigma_g^2}{\bar{I}_D}\right)^{nL_D} \tag{14a}$$

$$\Upsilon_4 = \left(\frac{I_{\max}\sigma_g^2}{n\sigma_{f_{rp}}^2}\right)\left(\frac{P_r\sigma_g^2}{\bar{I}_D}\right)^{nL_D} e^{-\frac{I_{\max}}{P_r\sigma_{f_{rp}}^2}} \tag{14b}$$

$$\delta = \frac{P_r\sigma_g^2}{n} \tag{14c}$$

$$\eta = \frac{P_r\sigma_g^2}{\bar{I}_D}. \tag{14d}$$

Then, the tight approximate per-hop equivalent cdf of the first and second hops can be written as in (15) and (16), shown at the bottom of the next page, respectively. It is worth mentioning that these notations have been carefully chosen, so that the first- and second-hop equations look similar in structure. However, the notations for each hop are different; therefore, the same procedure of derivation can applied to the error probability and

$$F_{\gamma_h^{\rm eff}}(\gamma) = 1 - \left[e^{-\frac{\gamma}{P_s\sigma_h^2}}\left(\frac{P_s\sigma_h^2}{P_s\sigma_h^2+\gamma\bar{I}_R}\right)^{L_R}\left(1-e^{-\frac{I_{\max}}{P_s\sigma_{f_{sp}}^2}}\right) + \left(\frac{I_{\max}\sigma_h^2}{I_{\max}\sigma_h^2+\gamma\sigma_{f_{sp}}^2}\right)\left(\frac{I_{\max}\sigma_h^2+\gamma\sigma_{f_{sp}}^2}{\gamma\bar{I}_R\sigma_{f_{sp}}^2}\right)^{L_R} e^{\frac{I_{\max}\sigma_h^2+\gamma\sigma_{f_{sp}}^2}{\gamma\bar{I}_R\sigma_{f_{sp}}^2}} \times \Gamma\left(1-L_R, \left(\frac{I_{\max}\sigma_h^2+\gamma\sigma_{f_{sp}}^2}{\gamma\bar{I}_R\sigma_{f_{sp}}^2}\right)\left(\frac{P_s\sigma_h^2+\gamma\bar{I}_R}{P_s\sigma_h^2}\right)\right)\right] \tag{8}$$

$$F_{\gamma_{g*}}(\gamma) = 1 - \sum_{n=1}^{K}\binom{K}{n}(-1)^{n+1}\left[e^{-\frac{n\gamma}{P_r\sigma_g^2}}\left(\frac{P_r\sigma_g^2}{P_r\sigma_g^2+\gamma\bar{I}_D}\right)^{nL_D}\left(1-e^{-\frac{I_{\max}}{P_r\sigma_{f_{rp}}^2}}\right) + \left(\frac{I_{\max}\sigma_g^2}{I_{\max}\sigma_g^2+n\gamma\sigma_{f_{rp}}^2}\right) \times \left(\frac{I_{\max}\sigma_g^2+n\gamma\sigma_{f_{rp}}^2}{\gamma\bar{I}_D\sigma_{f_{rp}}^2}\right)^{nL_D} e^{\frac{I_{\max}\sigma_g^2+n\gamma\sigma_{f_{rp}}^2}{\gamma\bar{I}_D\sigma_{f_{rp}}^2}}\Gamma\left(1-nL_D, \left(\frac{I_{\max}\sigma_g^2+n\gamma\sigma_{f_{rp}}^2}{\gamma\bar{I}_D\sigma_{f_{rp}}^2}\right)\left(\frac{P_r\sigma_g^2+\gamma\bar{I}_D}{P_r\sigma_g^2}\right)\right)\right] \tag{9}$$

TABLE I
COMPARISON BETWEEN THE EXACT AND APPROXIMATE REPRESENTATIONS OF THE EXPONENTIAL INTEGRAL FUNCTION

$I_{\max}$	$P_s = 10$ dB		$P_s = 15$ dB	
	Exact	Approximate	Exact	Approximate
4	0.194939388	0.184211969	0.207475405	0.194783537
8	0.104513633	0.102612305	0.112473998	0.110134216
12	0.048781832	0.04856972	0.052923924	0.052654999
16	0.020926427	0.020908823	0.02280764	0.022784929
20	0.008603787	0.008602534	0.009397708	0.009396079
24	0.00347106	0.003470977	0.003794922	0.003794814
28	0.001389295	0.001389289	0.001519509	0.001519502
32	0.000554279	0.000554279	0.000606325	0.000606324

ergodic capacity for one hop to the other with the condition of replacing the notations that have been defined for a particular hop.

Proof: See Appendix B.

It is worth noting that the proposed tight approximation does not have a significant impact on the analytical calculations and gives quite accurate results, particularly for the case of ($I_{\max} \geq P_s$ and P_r). It is obvious that in the case when $I_{\max} < P_s$ and P_r (i.e., $I_{\max}$ dominant system), the secondary transmitters cannot take full advantage of their transmission power limits, and in this case, an error floor is expected in the system performance. The accuracy of the proposed tight approximation can be observed later from the Monte Carlo simulations and numerical results. For instance, in Fig. 2, we have plotted the outage probability using the derived tight approximate cdf equations. It can be observed that our proposed tight approximation gives quite accurate results in comparison to the exact results. In addition, the approximation has been applied only to one term in the cdf formula. Moreover, we have constructed Table I for the purpose of comparison between the exact and tight approximate values of the exponential integral function term that we have proposed in the cdf formula.

1) Error Probability for the First Hop: The first-hop error probability is derived as follows.

Corollary 2: The first-hop average error probability can be obtained as in (17), shown at the bottom of the page, where $U(a,b,z)$ is the confluent hypergeometric function defined in [41, eq. (13.2.5)], and erfc(.) is the complementary error function defined in [42, eq. (7.2.2)]. Moreover, the values of λ_{1_i}, λ_2, and λ_3 are calculated by using the following equations:

$$\lambda_{1_i} = \frac{1}{(L_R-1-i)!}\frac{\partial^{L_R-1-i}}{\partial z^{L_R-1-i}}\frac{1}{(\Lambda_1+z)(\Lambda_2+z)}\bigg|_{z=-\beta} \tag{18a}$$

$$\lambda_2 = (\beta-\Lambda_1)^{1-L_R}(\Lambda_2-\Lambda_1)^{-1} \tag{18b}$$

$$\lambda_3 = (\beta-\Lambda_2)^{1-L_R}(\Lambda_1-\Lambda_2)^{-1}. \tag{18c}$$

Proof: See Appendix C.

2) Error Probability for the Opportunistic Second Hop: The same procedure can be repeated to derive the average error probability of the second hop. The only difference is that we use the tight approximate opportunistic cdf for the second hop that we derived in (16). For the purpose of saving space, we have omitted the equations.

Finally, the end-to-end error probability can be calculated by substituting the calculated per-hop error probability into (12).

C. Approximate CDF of the SINR $\gamma_{\text{eq}}^{\text{opp}}$

Although the expression for $F_{\gamma_{\text{eq}}^{\text{opp}}}(\gamma)$ allows for a numerical evaluation of the system performance, it may not be computationally intensive and does not offer insight into the effect of the system parameters. Now, we aim to express $F_{\gamma_{\text{eq}}^{\text{opp}}}(\gamma)$ and $\bar{P}_b(e)$ in simpler forms. To get more accurate results, we re-represent the exponential integral function in more detailed terms. This can be obtained by using [41, eq. (5.1.14)].

It is widely known that the asymptotic error probability can be derived based on the behavior of the cdf of the output SINR around the origin. By using Taylor's series and considering $P_s, P_r < I_{\max}$, $F_{\gamma_{\text{eq}}^{\text{opp}}}(\gamma)$ can be rewritten as

$$F_{\gamma_{\text{eq}}^{\text{opp}}}(\gamma) \approx \left(\frac{(1+L_R\bar{I}_R)}{P_s\sigma_h^2} + \frac{\sigma_{f_{sp}}^2}{I_{\max}\sigma_h^2}e^{-\frac{I_{\max}}{P_s\sigma_{f_{sp}}^2}} + \sum_{n=1}^{K}\binom{K}{n}\right.$$
$$\left.\times(-1)^{n+1}\left(\frac{n(1+L_D\bar{I}_D)}{P_r\sigma_g^2} + \frac{n\sigma_{f_{rp}}^2}{I_{\max}\sigma_g^2}e^{-\frac{I_{\max}}{P_r\sigma_{f_{rp}}^2}}\right)\right)\gamma. \tag{19}$$

$$F_{\gamma_h^{\text{eff}}}^{\text{app}}(z) = 1 - e^{-\frac{z}{\alpha}}\left[\frac{\Upsilon_1}{(\beta+z)^{L_R}} + \frac{\Upsilon_2}{(\beta+z)^{L_R-1}\times(\Lambda_1+z)\times(\Lambda_2+z)}\right] \tag{15}$$

$$F_{\gamma_{g*}}^{\text{app}}(z) = 1 - \sum_{n=1}^{K}\binom{K}{n}(-1)^{n+1}e^{-\frac{z}{\delta}}\left[\frac{\Upsilon_3}{(\eta+z)^{L_D}} + \frac{\Upsilon_4}{(\eta+z)^{L_D-1}\times(\Lambda_3+z)\times(\Lambda_4+z)}\right] \tag{16}$$

$$\bar{P}_b^{sr}(e) = \frac{a}{2} - \frac{a}{2}\left[\Upsilon_1\sqrt{b}\beta^{\frac{1}{2}-L_R}U\left(\frac{1}{2},\frac{3}{2}-L_R,\beta\left(b+\frac{1}{\alpha}\right)\right) + \Upsilon_2\sqrt{b}\times\left\{\sum_{i=1}^{L_R-1}\lambda_{1_i}\beta^{\frac{1}{2}-i}U\left(\frac{1}{2},\frac{3}{2}-i,\beta\left(b+\frac{1}{\alpha}\right)\right)\right.\right.$$
$$\left.\left.+\lambda_2\sqrt{\frac{\pi}{\Lambda_1}}e^{\left(b+\frac{1}{\alpha}\right)\Lambda_1}\operatorname{erfc}\left(\sqrt{\left(b+\frac{1}{\alpha}\right)\Lambda_1}\right) + \lambda_3\sqrt{\frac{\pi}{\Lambda_2}}e^{\left(b+\frac{1}{\alpha}\right)\Lambda_2}\operatorname{erfc}\left(\sqrt{\left(b+\frac{1}{\alpha}\right)\Lambda_2}\right)\right\}\right] \tag{17}$$

Therefore, the average error probability can be written as

$$\bar{P}_b(e) \approx \frac{a}{2b}\left(\frac{(1+L_R\bar{I}_R)}{P_s\sigma_h^2} + \frac{\sigma_{f_{sp}}^2}{I_{\max}\sigma_h^2}e^{-\frac{I_{\max}}{P_s\sigma_{f_{sp}}^2}} + \sum_{n=1}^{K}\binom{K}{n}\right.$$
$$\left.\times(-1)^{n+1}\left(\frac{n(1+L_D\bar{I}_D)}{P_r\sigma_g^2} + \frac{n\sigma_{f_{rp}}^2}{I_{\max}\sigma_g^2}e^{-\frac{I_{\max}}{P_r\sigma_{f_{rp}}^2}}\right)\right). \quad (20)$$

From (19), we would like to inspect the diversity gain of the secondary network. According to [43], at the high-SNR regime (i.e., $\gamma \to \infty$), the outage probability formula can be written as

$$P_{\text{out}} \approx (O_c\gamma)^{-G_d} \quad (21)$$

where G_d and O_d are the diversity gain and the coding gain, respectively. Now, by comparing (19) with (21), we can see that $G_d = 1$.

The result in (20) confirms that opportunistic scheduling has no impact on the diversity gain. However, by inspecting (20), we see that the effect of opportunistic scheduling is to increase the array gain [10]. Furthermore, the performance for $K > 1$ is dominated by the $S - R$ channel. Note that when $I_{\max} \to \infty$, we have the same widely known asymptotic expression for ordinary dual-hop DF networks, which validates our obtained results.

D. Ergodic Capacity

Another important performance indicator for the wireless communication network is ergodic capacity [20]. It can be defined as the maximum capacity data rate that the system can achieve. To assess the CR network capacity, it is important to know the achievable throughput of the system. The ergodic capacity can be mathematically obtained by taking the expectation of the average equivalent SNR. Furthermore, it can be calculated by using the equivalent cdf of the system [20] and can be represented as

$$C_{erg} = \int_0^\infty \frac{\bar{F}_{\gamma_{\text{eq}}}(x)}{1+x}dx \quad (22)$$

where $\bar{F}_{\gamma_{\text{eq}}}(x)$ is the complementary cdf. Then, the end-to-end ergodic capacity can be obtained by using the following formula:

$$C_{erg}^{e2e} = \min\left(C_{erg}^{sr}, C_{erg}^{g^*}\right) \quad (23)$$

where C_{erg}^{sr} and $C_{erg}^{g^*}$ are the ergodic capacities of the first hop and the opportunistic second hop, respectively. Here, we derive the ergodic capacity for the second hop.

Corollary 3: The second-hop ergodic capacity formula can be expressed as in (24), shown at the bottom of the page.

Proof: See Appendix D.

In (24), $E_1(x)$ is the exponential integral function defined in [42, eq. (6.2.6)]. Furthermore, the values of $\omega_{g1_{r_3}}$, ω_{g2}, $\omega_{g3_{r_4}}$, ω_{g4}, ω_{g5}, and ω_{g6} are calculated by using (25a)–(25f), respectively. Thus

$$\omega_{g1_{r_3}} = \frac{1}{(nL_D - r_3)!}\frac{\partial^{nL_D - r_3}}{\partial z^{nL_D - r_3}}(1+z)^{-1}\bigg|_{z=-\eta} \quad (25a)$$

$$\omega_{g2} = (\eta - 1)^{-nL_D} \quad (25b)$$

$$\omega_{g3_{r_4}} = \frac{1}{(nL_D - 1 - r_4)!} \times \frac{\partial^{nL_D-1-r_4}}{\partial z^{nL_D-1-r_4}}(1+z)^{-1}(\Lambda_3+z)^{-1}(\Lambda_4+z)^{-1}\bigg|_{z=-\eta} \quad (25c)$$

$$\omega_{g4} = (\eta - 1)^{1-nL_D}(\Lambda_3 - 1)^{-1}(\Lambda_4 - 1)^{-1} \quad (25d)$$

$$\omega_{g5} = (\eta - \Lambda_3)^{1-nL_D}(1 - \Lambda_3)^{-1}(\Lambda_4 - \Lambda_3)^{-1} \quad (25e)$$

$$\omega_{g6} = (\eta - \Lambda_4)^{1-nL_D}(1 - \Lambda_4)^{-1}(\Lambda_3 - \Lambda_4)^{-1}. \quad (25f)$$

For the first-hop ergodic capacity formula, we first substitute the derived tight approximate first-hop complementary cdf (i.e., $F_{\gamma_h^{\text{eff}}}^{\text{app}}(z)$) from (15) into (22). Then, we get an integral formula that has two main parts. It can be observed that these two parts are quite similar to the two parts in the second-hop ergodic capacity formula derived in Appendix D; we only need to replace δ, η, Λ_3, Λ_4, Υ_3, and Υ_4 with α, β, Λ_1, Λ_2, Υ_1, and Υ_2, respectively.

E. Optimum Power Allocation for $K = 1$

Since only when $K = 1$, both channels $S - R$ and $R - D_1$ have the same impact. Here, aiming for improved system performance, we study adaptive power allocation subject to a sum-power constraint, i.e., $P_s + P_r = P_t$, where P_t is the total given power. The optimization problem can be formulated as

$$P_s^*, P_r^* = \arg\min_{P_s, P_r}\ \bar{P}_b(e)$$
$$\text{subject to}\quad P_s + P_r = P_t \ \text{ and } \ P_s, P_r > 0. \quad (26)$$

By taking the second derivative of $\bar{P}_b(e)$ with respect to P_s, it is easy to see that $\partial^2\bar{P}_b(e)/\partial P_s^2$ is positive in the interval $P_s \in \{0, P_t\}$. This implies that the objective function is a

$$C_{erg}^{g^*} = \sum_{n=1}^{K}\binom{K}{n}(-1)^{n+1}\left\{\Upsilon_3\left[\sum_{r_3=1}^{nL_D}\omega_{g1_{r_3}}\eta^{1-r_3}e^{\frac{\eta}{\delta}}E_{r_3}\left(\frac{\eta}{\delta}\right) + \omega_{g2}e^{\frac{1}{\delta}}E_1\left(\frac{1}{\delta}\right)\right]\right.$$
$$\left. + \Upsilon_4\left[\sum_{r_4=1}^{nL_D-1}\omega_{g3_{r_4}}\eta^{1-r_4}e^{\frac{\eta}{\delta}}E_{r_4}\left(\frac{\eta}{\delta}\right) + \omega_{g4}e^{\frac{1}{\delta}}E_1\left(\frac{1}{\delta}\right) + \omega_{g5}e^{\frac{\Lambda_3}{\delta}}E_1\left(\frac{\Lambda_3}{\delta}\right) + \omega_{g6}e^{\frac{\Lambda_4}{\delta}}E_1\left(\frac{\Lambda_4}{\delta}\right)\right]\right\} \quad (24)$$

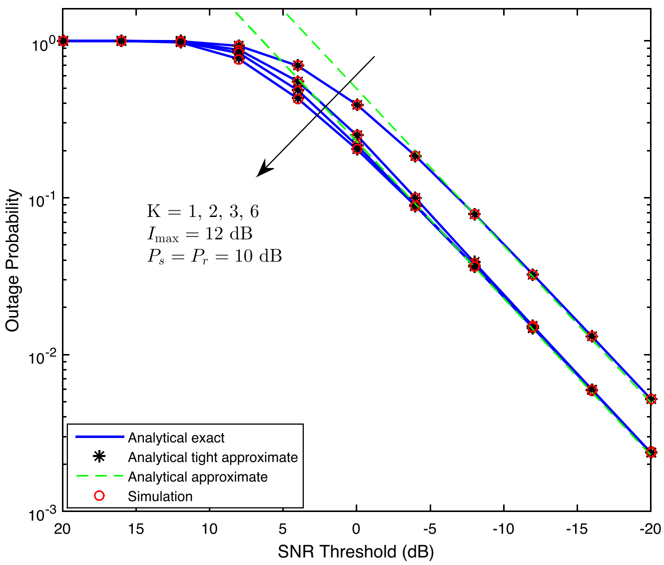

Fig. 2. Outage probability for different numbers of destination users.

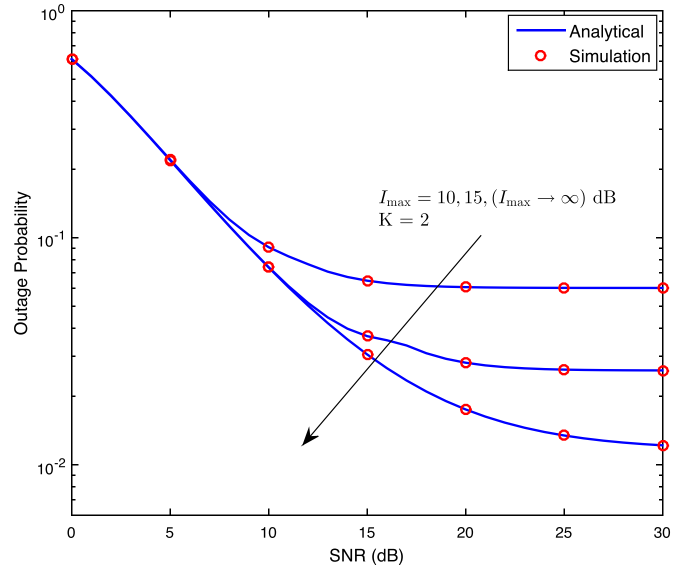

Fig. 3. Outage probability for different $I_{\max}$ values.

strictly convex function of P_s in $\{0, P_t\}$. Hence, taking the first derivative of $\bar{P}_b(e)$ in (20) with respect to P_s and setting it to zero, we can find the optimal power allocation solution. Specifically, the optimal source power P_s^* is the root of the following equation:

$$\frac{1 + L_D\bar{I}_D - e^{-\frac{I_{\max}}{(P_t - P_s)\sigma_{f_{rp}}^2}}}{\sigma_g^2(P_t - P_s)^2} = \frac{1 + L_R\bar{I}_R - e^{-\frac{I_{\max}}{P_s\sigma_{f_{sp}}^2}}}{P_s^2\sigma_h^2}. \quad (27)$$

The optimal relay power is given by $P_r^* = P_t - P_s^*$. It is difficult to find a closed-form expression for the optimal source power, i.e., P_s^*. However, a numerical solution can be found by standard iterative root-finding algorithms, such as the bisection method and Newton's method, with great efficiency. However, if we assume $P_s, P_r \ll I_{\max}$ [20] and after some mathematical manipulations, the closed-form expressions for these optimal power values can be found as

$$P_s^* \approx \left[\frac{\sqrt{\sigma_g^2(1 + L_R\bar{I}_R)}}{\sqrt{\sigma_g^2(1 + L_R\bar{I}_R)} + \sqrt{\sigma_h^2(1 + L_D\bar{I}_D)}}\right] P_t \quad (28a)$$

$$P_r^* \approx \left[\frac{\sqrt{\sigma_h^2(1 + L_D\bar{I}_D)}}{\sqrt{\sigma_h^2(1 + L_D\bar{I}_D)} + \sqrt{\sigma_g^2(1 + L_R\bar{I}_R)}}\right] P_t. \quad (28b)$$

In previous optimal power calculations, both optimal calculated power values P_s^* and P_r^* should satisfy the criteria of the protection of the QoS of the primary receiver. For example, the actual transmit power at the secondary source node should satisfy the following criteria: $(E_{us} = \min((I_{\max}/|f_{sp}|^2), P_s^*))$. Similarly, for the optimal power at the relay node, the actual relay transmit power should satisfy these criteria: $(E_{ur} = \min((I_{\max}/|f_{rp}|^2), P_r^*))$. Therefore, a guarantee of protection of the QoS of the primary user should always be provided.

In the scenario where any of the calculated optimal power values are above the interference power constraint (i.e., $I_{\max}$ dominates the transmission power limits), an error floor occurs in the secondary system performance results. This is because the secondary transmitters cannot take full advantage of their transmission power limits.

Finally, it is worth mentioning that although numerical calculation is at the source, the complexity of the proposed algorithm is very low, since the computations are needed only once for each system configuration. This is due to the fact that our analysis is based on average values rather than instantaneous values that, in practice, can be obtained through long-term averaging of the received signal power.

IV. Numerical Results

For the purpose of illustration and to validate the derived mathematical works, we present some numerical and Monte Carlo simulation examples.

In Fig. 2, the outage probability has been plotted to show the effect of opportunistic scheduling. We have set the CCI power values to $\bar{I}_R = 3$ dB, $\bar{I}_D = 2$ dB, and $L_R = L_D = 2$. It can be observed that opportunistic scheduling has less impact on the system performance when $K > 1$ due to the fact that the source–relay link will dominate the performance characteristic.

Fig. 3 shows the outage probability for different values of $I_{\max}$. The network parameter values for this figure are chosen as follows: The SNR threshold is 1 dB, and the CCI power values $\bar{I}_R$ and $\bar{I}_D$ are 0.01 of the effective or actual transmit power values at the secondary source and relay node (i.e., E_{us} and E_{ur}) and $L_R = L_D = 2$. It can be observed that even if there is no interference power constraint (i.e., $I_{\max} \to \infty$), there is an outage floor. This is because of the linear increase in the CCI power with respect to the effective transmission power values at the source and relay nodes. From this, we can see how the CCI degrades the performance of the system.

Fig. 4 shows the ergodic capacity for different $I_{\max}$, K, and CCI power values. The network parameter values for this figure are chosen as follows: The CCI exists at the relay and destination nodes where $L_R = L_D = 2$, as well as for the case

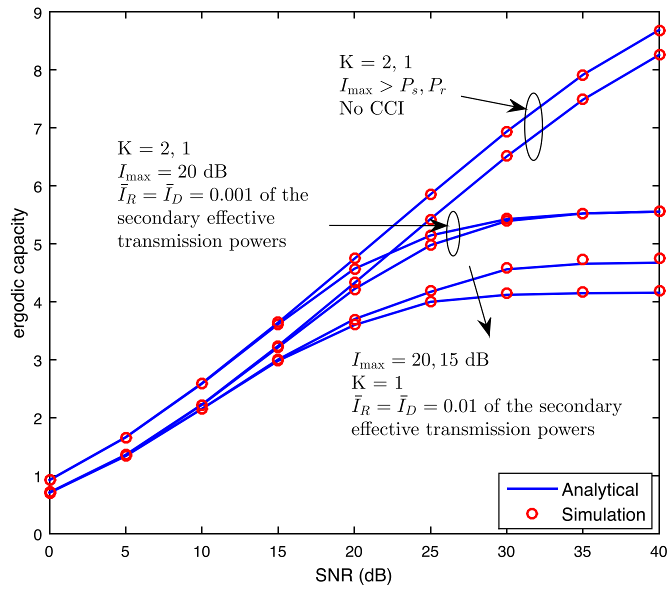

Fig. 4. Ergodic capacity for different values of $I_{\max}$, K, and CCI power.

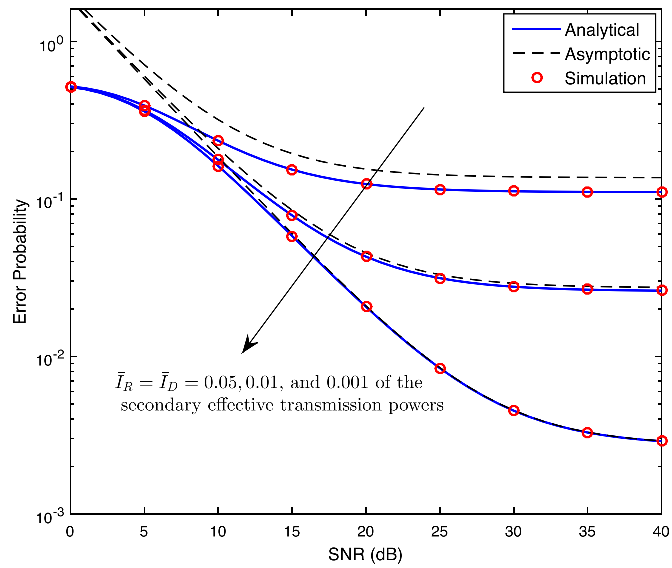

Fig. 6. Error probability for different values of CCI power.

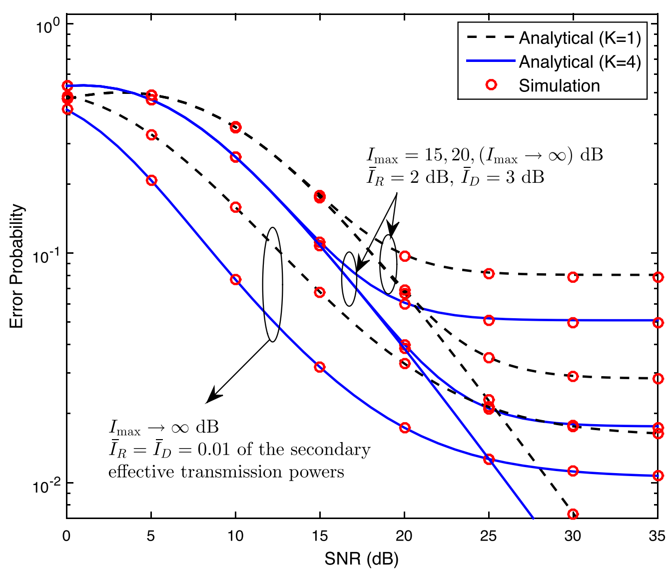

Fig. 5. Error probability for different values of $I_{\max}$ and K.

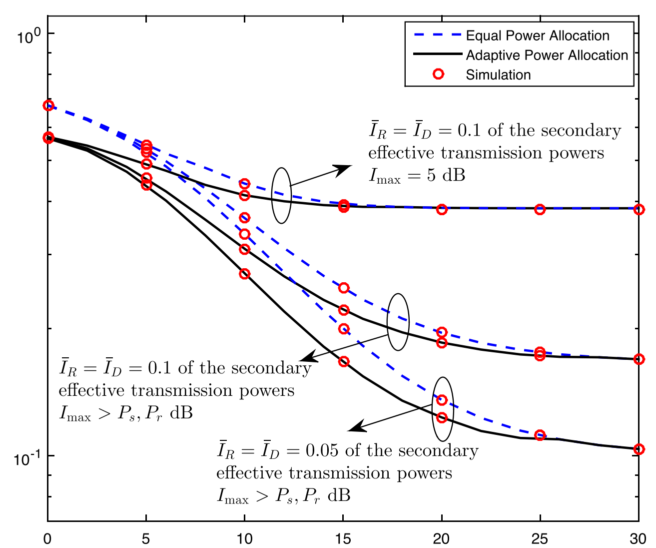

Fig. 7. Performance of the optimal power allocation algorithm in comparison to the equal power allocation.

where there is no CCI and $I_{\max}$. From the results, it can be deduced that both the CCI and $I_{\max}$ will degrade the system performance. For example, for a single destination user $K = 1$, when both $I_{\max}$ and CCI have an impact on the secondary network (i.e., $I_{\max} = 15$ dB and $\bar{I}_R = \bar{I}_D = 0.01 \times E_{us}, E_{ur}$), capacity saturation occurs at 30 dB, and the performance cannot improve better than 4.1 bits/s/Hz, even when the transmission power increased further. However, when these performance limitations are not present, it is possible to reach 6.5 bits/s/Hz at 30 dB.

Fig. 5 shows the error probability versus the total transmission power for different $I_{\max}$ and K values. The network parameter values for this figure are chosen as follows: The CCI power values $\bar{I}_R$ and $\bar{I}_D$ have fixed values and also linearly increase with the effective transmission power values by the ratio of 0.01, and $L_R = 3$, $L_D = 1$. In the figure, we can see that higher $I_{\max}$ will lead to better performance. In addition, the error floor in this case is due to both $I_{\max}$ and CCI. Moreover, in a specific region, even for a high value of $I_{\max}$, an error floor can be observed, which is due to the CCI power.

For the purpose of only showing the impact of the CCI power on the error probability performance of the CR network, Fig. 6 has been plotted, which is the error probability versus the total transmission power for different CCI power values. The network parameter values for this figure are chosen as follows: $K = 2$, $L_R = 2$, $L_D = 3$, and $I_{\max} > P_s, P_r$. The error floor in this case is completely due to the impact of CCI power. For example, when the rate of increase of the CCI power with respect to the effective secondary transmission power values is 0.05, the error performance saturates at 0.11, which means that the error probability performance cannot improve further, even if the transmission power increases.

In Fig. 7, the performance of the optimal power allocation in comparison with the equal power allocation for the case when $K = 1$ for different CCI power values and $I_{\max}$ is shown. With the help of (27) and by using the bisection method, the optimal power values P_s^* and P_r^* were calculated. It can be observed that optimal power allocation leads to an improved performance in comparison with equal power allocation. Moreover, when $I_{\max}$ limits the secondary transmission power and the CCI power is relatively high, the improvement in the error performance due to the optimal power allocation scheme is less significant.

V. Conclusion

In this paper, a comprehensive study of the performance analysis of the opportunistic dual-hop multiuser DF underlay cognitive cooperative network in the presence of CCI has been presented. An exact closed-form expression for the cdf of the equivalent SINR has been derived, and the exact outage probability has been investigated. In turn, a tight approximate cdf has been proposed. Based on this, expressions for the average error probability and the system ergodic capacity over the Rayleigh fading channel have been derived. In addition, simple approximate expressions for the outage probability and the average error probability have been obtained.

Finally, we investigated the system power optimization to minimize the system error probability. Numerical results and Monte Carlo simulations using MATLAB have also been presented to validate the correctness of the analytical results. Our results showed that applying the opportunistic scheduling can improve the CR system performance. On the other hand, CCI and the $I_{\max}$ consideration will cause its degradation.

It is worth mentioning that our approach can be easily extended to the multihop cognitive cooperative network. For instance, the outage probability can be obtained by simply substituting the per-hop results into [38, eq. (8)]. In addition, the error probability and the ergodic capacity can be calculated by substituting the per-hop results into [29, eqs. (28) and (47)], respectively.

Appendix A
First-Hop Exact Cumulative Distribution Function Derivation Steps

Recall that the effective SINR for the first hop can be written as $\gamma_h^{\text{eff}} = \gamma_h/(1 + \sum_{j=1}^{L_R} I_{Rj})$; hence, considering both the source node power constraint and the interference power constraint, we can rewrite the given formula as

$$\gamma_h^{\text{eff}} = \min\left(\frac{I_{\max}}{X}, P_s\right)\left(\frac{Y}{1+Z}\right) \tag{29}$$

where X, Y, and Z represent the RVs $|f_{sp}|^2$, $|h|^2$, and $\sum_{j=1}^{L_R} I_{R_j}$, respectively. Since we have assumed that all the channels follow Rayleigh fading distribution, the pdf of X has an exponential distribution and is written as: $f_X(x) = (1/\sigma_{f_{sp}}^2)\exp(-(x/\sigma_{f_{sp}}^2))$. In addition, the corresponding cdf can be written as: $F_X(x) = 1 - \exp(-(x/\sigma_{f_{sp}}^2))$. We first derive the equivalent cdf of $Y/(1+Z)$. Let W represent the resulting RV of this combination $W = Y/(1+Z)$. Therefore, the cdf of W can be written as

$$F_W(\gamma) = \int_{z=0}^{\infty} F_Y\left((z+1)\gamma\right) f_Z(z) dz \tag{30}$$

where $F_Y(\gamma)$ is the cdf of the channel gain between the source and relay node that can be expressed as $F_Y(y) = 1 - \exp(-(y/\sigma_h^2))$. $f_Z(z)$ is the pdf of RV $\sum_{j=1}^{L_R} I_{R_j}$ that can be expressed as $f_Z(z) = (z^{L_R-1}/\bar{I}_R^{L_R}\Gamma(L_R))\exp(-(z/\bar{I}_R))$, where $\bar{I}_R$ is the average INR. By substituting both formulas of $F_Y(y)$ and $f_Z(z)$ into (30), we get the cdf of RV W, i.e.,

$$F_W(\gamma) = 1 - e^{-\frac{\gamma}{\sigma_h^2}}\left(\frac{\sigma_h^2}{\sigma_h^2 + \gamma\bar{I}_R}\right)^{L_R}. \tag{31}$$

It is well known that the cdf of γ_h^{eff} can be obtained by

$$F_{\gamma_h^{\text{eff}}}(\gamma) = \Pr\left(\gamma_h^{\text{eff}} \le \gamma\right). \tag{32}$$

Then, with the help of the total probability theorem, the cdf of $F_{\gamma_h^{\text{eff}}}(\gamma)$ can be expressed by the following formula:

$$F_{\gamma_h^{\text{eff}}}(\gamma) = \Pr\left(\frac{I_{\max}}{X}W \le \gamma, \frac{I_{\max}}{X} < P_s\right) + \Pr\left(P_s W \le \gamma, \frac{I_{\max}}{X} > P_s\right). \tag{33}$$

The given formula can be represented in terms of the integrals, i.e.,

$$\begin{aligned} F_{\gamma_h^{\text{eff}}}(\gamma) &= \int_{x=\frac{I_{\max}}{P_s}}^{\infty} \int_{y=0}^{\frac{\gamma x}{I_{\max}}} f_X(x) f_W(y) dx\, dy \\ &\quad + \int_{x=0}^{\frac{I_{\max}}{P_s}} \int_{y=0}^{\frac{\gamma}{P_s}} f_X(x) f_W(y) dx\, dy \\ &= I_1 + I_2. \end{aligned} \tag{34}$$

The second part of the given integrals (i.e., I_2) can be easily obtained as

$$I_2 = \left(1 - \left(\frac{\sigma_h^2}{\bar{I}_R}\right)^{L_R} \frac{e^{-\frac{\gamma}{P_s\sigma_h^2}}}{\left(\frac{\sigma_h^2}{\bar{I}_R} + \frac{\gamma}{P_s}\right)^{L_R}}\right)\left(1 - e^{-\frac{I_{\max}}{P_s\sigma_{f_{sp}}^2}}\right). \tag{35}$$

Moreover, the first part (i.e., I_1) can be written as

$$I_1 = \int_{x=\frac{I_{\max}}{P_s}}^{\infty} \frac{1}{\sigma_{f_{sp}}^2} e^{-\frac{x}{\sigma_{f_{sp}}^2}} \times \left(1 - \left(\frac{\sigma_h^2}{\bar{I}_R}\right)^{L_R} \frac{e^{-\frac{\gamma x}{I_{\max}\sigma_h^2}}}{\left(\frac{\sigma_h^2}{\bar{I}_R} + \frac{\gamma x}{I_{\max}}\right)^{L_R}}\right) dx. \tag{36}$$

After some arrangements, we can write the given formulas as

$$I_1 = e^{-\frac{I_{\max}}{P_s \sigma_{f_{sp}}^2}} - \left(\frac{I_{\max}\sigma_h^2}{\gamma \bar{I}_R}\right)^{L_R} \frac{1}{\sigma_{f_{sp}}^2} \int_{x=\frac{I_{\max}}{P_s}}^{\infty} \frac{e^{-x\left(\frac{\gamma}{I_{\max}\sigma_h^2} + \frac{1}{\sigma_{f_{sp}}^2}\right)}}{\left(\frac{I_{\max}\sigma_h^2}{\gamma \bar{I}_R} + x\right)^{L_R}} dx. \tag{37}$$

Now, let $t = (I_{\max}\sigma_h^2/\gamma \bar{I}_R) + x$; therefore, we get

$$I_1 = e^{-\frac{I_{\max}}{P_s \sigma_{f_{sp}}^2}} - \left(\frac{I_{\max}\sigma_h^2}{\gamma \bar{I}_R}\right)^{L_R} \frac{1}{\sigma_{f_{sp}}^2} e^{\left(\frac{\gamma \sigma_{f_{sp}}^2 + I_{\max}\sigma_h^2}{I_{\max}\sigma_h^2 \sigma_{f_{sp}}^2}\right)\left(\frac{I_{\max}\sigma_h^2}{\gamma \bar{I}_R}\right)} \times \int_{t=\frac{I_{\max}}{P_s} + \frac{I_{\max}\sigma_h^2}{\gamma \bar{I}_R}}^{\infty} \frac{e^{-t\left(\frac{\gamma \sigma_{f_{sp}}^2 + I_{\max}\sigma_h^2}{I_{\max}\sigma_h^2 \sigma_{f_{sp}}^2}\right)}}{t^{L_R}} dt. \tag{38}$$

Next, we change the variable in the given integral so that $s = t((\gamma \sigma_{f_{sp}}^2 + I_{\max}\sigma_h^2)/I_{\max}\sigma_h^2 \sigma_{f_{sp}}^2)$. After this substitution and by doing some straightforward mathematical manipulation and comparing our formula with [42, eq. (5.2.1)]), we can obtain the desired formula as

$$I_1 = e^{-\frac{I_{\max}}{P_s \sigma_{f_{sp}}^2}} - \left(\frac{I_{\max}\sigma_h^2}{I_{\max}\sigma_h^2 + \gamma \sigma_{f_{sp}}^2}\right)\left(\frac{I_{\max}\sigma_h^2 + \gamma \sigma_{f_{sp}}^2}{\gamma \bar{I}_R \sigma_{f_{sp}}^2}\right)^{L_R} \times e^{\frac{I_{\max}\sigma_h^2 + \gamma \sigma_{f_{sp}}^2}{\gamma \bar{I}_R \sigma_{f_{sp}}^2}} \Gamma\left(1 - L_R, \frac{\left(\gamma \bar{I}_R + P_s \sigma_h^2\right)\left(\gamma \sigma_{f_{sp}}^2 + I_{\max}\sigma_h^2\right)}{\gamma \sigma_{f_{sp}}^2 P_s \sigma_h^2 \bar{I}_R}\right). \tag{39}$$

Finally, an exact equivalent cdf expression for the first-hop equivalent SINR (i.e., $F_{\gamma_h^{\text{eff}}}(\gamma)$) can be obtained by combining both parts I_1 and I_2, which can be represented as in (8).

Appendix B
Proof of Theorem 1

The aim of this theorem is to provide a tight approximate representation of the derived per-hop cdfs, so that we can do further mathematical manipulation on them, for example, deriving the error probability and ergodic capacity formulas. Using [41, eq. (5.1.45)], the upper incomplete gamma function can be represented in terms of the exponential integral function as follows:

$$\Gamma(1-n, x) = x^{1-n} E_n(x) \tag{40}$$

where $E_n(x)$ is the exponential integral function defined in [42, eq. (8.19.2)]. After this substitution, the cdf of the first hop can be written as in (41), shown at the bottom of the page.

According to [42, eq. (8.19.21)], the exponential integral function can be bounded as

$$\frac{1}{x+n} < e^x E_n(x) \leq \frac{1}{x+n-1}. \tag{42}$$

Furthermore, we apply the following approximation for the exponential integral function:

$$E_n(x) \approx \frac{e^{-x}}{x+n}. \tag{43}$$

The next step is to substitute the notations in (13a)–(13d) into the cdf formula in (41) and then apply the proposed approximate formula in (43). After doing some mathematical manipulations and arrangements, we get our desired and simpler formula, which is a tight approximate cdf of the first-hop equivalent SINR and is represented in (15), where Λ_1 and Λ_2 are obtained by using the formulas given in (44a) and (44b), shown below, respectively. Thus

$$\Lambda_1 = \frac{\sigma_h^2}{2}\left[\left(P_s L_R + \frac{I_{\max}}{\sigma_{f_{sp}}^2} + \frac{P_s}{\bar{I}_R}\right) + \sqrt{(P_s L_R)^2 + 2P_s L_R\left(\frac{I_{\max}}{\sigma_{f_{sp}}^2} + \frac{P_s}{\bar{I}_R}\right) + \left(\frac{I_{\max}}{\sigma_{f_{sp}}^2} - \frac{P_s}{\bar{I}_R}\right)^2}\right] \tag{44a}$$

$$\Lambda_2 = \frac{\sigma_h^2}{2}\left[\left(P_s L_R + \frac{I_{\max}}{\sigma_{f_{sp}}^2} + \frac{P_s}{\bar{I}_R}\right) - \sqrt{(P_s L_R)^2 + 2P_s L_R\left(\frac{I_{\max}}{\sigma_{f_{sp}}^2} + \frac{P_s}{\bar{I}_R}\right) + \left(\frac{I_{\max}}{\sigma_{f_{sp}}^2} - \frac{P_s}{\bar{I}_R}\right)^2}\right]. \tag{44b}$$

The same procedure that we used for the first-hop cdf can be repeated for the opportunistic second-hop cdf. Therefore, we can formulate a tight approximate opportunistic cdf of the second-hop opportunistic equivalent SINR as in (16), where Λ_3

$$F_{\gamma_h^{\text{eff}}}(z) = 1 - \left[e^{-\frac{z}{P_s \sigma_h^2}}\left(\frac{P_s \sigma_h^2}{P_s \sigma_h^2 + z\bar{I}_R}\right)^{L_R}\left(1 - e^{-\frac{I_{\max}}{P_s \sigma_{f_{sp}}^2}}\right) + e^{\frac{I_{\max}\sigma_h^2 + z\sigma_{f_{sp}}^2}{z\bar{I}_R \sigma_{f_{sp}}^2}} E_{L_R}\left(\frac{I_{\max}\sigma_h^2 + z\sigma_{f_{sp}}^2}{z\bar{I}_R \sigma_{f_{sp}}^2}\frac{P_s \sigma_h^2 + z\bar{I}_R}{P_s \sigma_h^2}\right) \times \left(\frac{P_s \sigma_h^2}{P_s \sigma_h^2 + z\bar{I}_R}\right)^{L_R}\left(\frac{P_s \sigma_h^2 + z\bar{I}_R}{P_s \sigma_h^2}\right)\left(\frac{I_{\max}\sigma_h^2}{z\bar{I}_R \sigma_{f_{sp}}^2}\right)\right] \tag{41}$$

and Λ_4 are obtained by using the formulas given in (45a) and (45b), shown below, respectively. Thus

$$\Lambda_3 = \frac{\sigma_g^2}{2}\left[\left(P_r L_D + \frac{I_{\max}}{n\sigma_{f_{rp}}^2} + \frac{P_r}{\bar{I}_D}\right) + \sqrt{(P_r L_D)^2 + 2P_r L_D\left(\frac{I_{\max}}{n\sigma_{f_{rp}}^2} + \frac{P_r}{\bar{I}_D}\right) + \left(\frac{I_{\max}}{n\sigma_{f_{rp}}^2} - \frac{P_r}{\bar{I}_D}\right)^2}\,\right] \tag{45a}$$

$$\Lambda_4 = \frac{\sigma_g^2}{2}\left[\left(P_r L_D + \frac{I_{\max}}{n\sigma_{f_{rp}}^2} + \frac{P_r}{\bar{I}_D}\right) - \sqrt{(P_r L_D)^2 + 2P_r L_D\left(\frac{I_{\max}}{n\sigma_{f_{rp}}^2} + \frac{P_r}{\bar{I}_D}\right) + \left(\frac{I_{\max}}{n\sigma_{f_{rp}}^2} - \frac{P_r}{\bar{I}_D}\right)^2}\,\right]. \tag{45b}$$

In Fig. 2, we have plotted the outage probability using the derived new expressions for cdf formulas and compared it with the exact results. It can be observed that our proposed tight approximation gives quite accurate results, particularly for the higher values of $I_{\max}$.

In addition, to show the accuracy of our proposed tight approximation numerically, we have constructed Table I, which is a comparison between the exact value of the exponential integral term and its corresponding tight approximated value. It will explain the tightness of the approximation that we have used in our analysis. For the exact calculation, we have calculated the value of $e^z E_{L_R}(z)$, where $z = ((I_{\max}\sigma_h^2 + \gamma_{th}\sigma_{f_{sp}}^2)/\gamma_{th}\bar{I}_R\sigma_{f_{sp}}^2)((P_s\sigma_h^2 + \gamma_{th}\bar{I}_R)/P_s\sigma_h^2)$. Furthermore, we have assumed the following values for the entities: $\sigma_h^2 = 2.2$, $\sigma_{f_{sp}}^2 = 0.7$, $\bar{I}_R = 3$ dB, $L_R = 2$, and $\gamma_{th} = 2$ dB. Moreover, for the tight approximate calculation, we have determined the value of $1/(L_R + z)$. The calculations have been made for different values of $I_{\max}$ in decibels and P_s.

APPENDIX C
FIRST-HOP AVERAGE ERROR PROBABILITY DERIVATION STEPS

For deriving the average bit error probability, we use a tight proposed approximated cdf in (15). After substituting (15) into (11), we get a formula that has three integral parts. In the following sections, we will discuss and/or derive each part. The first integral part can be easily obtained by comparing our formula with [42, eq. (5.2.1)]. Bearing in mind that $n! = \Gamma(n-1)$ and $\Gamma(1/2) = \sqrt{\pi}$, we have

$$\bar{P}_b^{sr1}(e) = \frac{a}{2}\sqrt{\frac{b}{\pi}}\int_0^\infty \frac{e^{-b\,x}}{\sqrt{x}}dx = \frac{a}{2} \tag{46}$$

where $\bar{P}_b^{sr1}(e)$ represents the first part of the first-hop average error probability formula. The second part of the integral has the following form:

$$\bar{P}_b^{sr2}(e) = -\frac{a}{2}\sqrt{\frac{b}{\pi}}\int_0^\infty \frac{e^{-b\,x}}{\sqrt{x}}\Upsilon_1\frac{e^{-\frac{x}{\alpha}}}{(\beta+z)^{L_R}}dx \tag{47}$$

where $\bar{P}_b^{sr2}(e)$ represents the second part of the first-hop average error probability formula. We exchange the variable in the given integral so that $t = x/\beta$; then, after performing some mathematical arrangements, we get

$$\bar{P}_b^{sr2}(e) = -\Upsilon_1\frac{a}{2}\sqrt{\frac{b}{\pi}}\beta^{\frac{1}{2}-L_R}\int_0^\infty \frac{e^{-t\beta\left(b+\frac{1}{\alpha}\right)}}{\sqrt{t}(1+t)^{L_R}}dt. \tag{48}$$

Using [41, eq. (13.2.5)], the desired formula can be obtained as

$$\bar{P}_b^{sr2}(e) = -\Upsilon_1\frac{a}{2}\sqrt{b}\beta^{-L_R+\frac{1}{2}}U\left(\frac{1}{2}, \frac{3}{2} - L_R, \beta\left(b + \frac{1}{\alpha}\right)\right). \tag{49}$$

The third part of the integral has the following form:

$$\bar{P}_b^{sr3}(e) = -\Upsilon_2\frac{a}{2}\sqrt{\frac{b}{\pi}}\int_0^\infty \frac{x^{-1/2}(\beta+x)^{1-L_R}e^{-bx}e^{-\frac{x}{\alpha}}}{(\Lambda_1+x)(\Lambda_2+x)}dx \tag{50}$$

where $\bar{P}_b^{sr3}(e)$ represents the third part of the first-hop average error probability formula. For the purpose of mathematical tractability and to simplify the given integral, we use the partial-fraction decomposition technique to represent the integral formula in a simpler form, i.e.,

$$\bar{P}_b^{sr3}(e) = -\Upsilon_2\frac{a}{2}\sqrt{\frac{b}{\pi}}\int_0^\infty \frac{e^{-x\left(b+\frac{1}{\alpha}\right)}}{\sqrt{x}} \times \left[\sum_{i=1}^{L_R-1}\frac{\lambda_{1_i}}{(\beta+x)^i} + \frac{\lambda_2}{(\Lambda_1+x)} + \frac{\lambda_3}{(\Lambda_2+x)}\right]dx \tag{51}$$

where λ_{1_i}, λ_2, and λ_3 are coefficient constants; their values are obtained by the formulas given in (18a)–(18c), respectively. Now, our formula has three parts; we define them as $\bar{P}_{b_1}^{sr3}(e)$, $\bar{P}_{b_2}^{sr3}(e)$, and $\bar{P}_{b_3}^{sr3}(e)$. By observing the integral formula, we deduce that $\bar{P}_{b_1}^{sr3}(e)$ is quite similar to the formula that we have derived in the previous section (i.e., second part of the error probability formula $\bar{P}_b^{sr2}(e)$). Therefore, it can be written as

$$\bar{P}_{b_1}^{sr3}(e) = -\Upsilon_2\frac{a}{2}\sqrt{b}\sum_{i=1}^{L_R-1}\lambda_{1_i}\beta^{\frac{1}{2}-i}U\left(\frac{1}{2}, \frac{3}{2}-i, \beta\left(b+\frac{1}{\alpha}\right)\right). \tag{52}$$

Moreover, the integral in $\bar{P}_{b_2}^{sr3}(e)$ can be solved as follows: First, we change the variable of the integral so that $x = \Lambda_1 t^2$. After doing this exchange operation and performing some mathematical arrangements, we get

$$\bar{P}_{b_2}^{sr3}(e) = -\frac{2\Upsilon_2\lambda_2}{\sqrt{\Lambda_1}}\frac{a}{2}\sqrt{\frac{b}{\pi}}\int_0^\infty \frac{e^{-\left(b+\frac{1}{\alpha}\right)\Lambda_1 t^2}}{(1+t^2)}dt. \tag{53}$$

By comparing our formula with [42, eq. (7.7.1)], we can get the desired form as

$$\bar{P}_{b_2}^{sr3}(e) = -\frac{a}{2}\Upsilon_2\lambda_2\sqrt{\frac{b\pi}{\Lambda_1}}e^{\left(b+\frac{1}{\alpha}\right)\Lambda_1}\text{erfc}\left(\sqrt{\left(b+\frac{1}{\alpha}\right)\Lambda_1}\right). \tag{54}$$

The derivation steps of the integral in $\bar{P}_{b_3}^{sr3}(e)$ are similar to previous derivations (i.e., $\bar{P}_{b_2}^{sr3}(e)$). Therefore, it can be written as

$$\bar{P}_{b_3}^{sr3}(e) = -\frac{a}{2}\Upsilon_2\lambda_3\sqrt{\frac{b\pi}{\Lambda_2}}e^{\left(b+\frac{1}{\alpha}\right)\Lambda_2}\text{erfc}\left(\sqrt{\left(b+\frac{1}{\alpha}\right)\Lambda_2}\right). \tag{55}$$

Finally, the average error probability for the first hop can be formulated by combining the three derived parts, and it can be written as in (17).

Appendix D
Second-Hop Opportunistic Ergodic Capacity Derivation Steps

After substituting the derived tight approximate opportunistic second-hop complementary cdf [i.e., $\bar{F}_{\gamma_{g*}}^{\text{app}}(z)$] from (16) into (22), we get an ergodic capacity formula that has two main parts; we name them $C_{erg_1}^{g*}$ and $C_{erg_2}^{g*}$, respectively. In the following sections, we derive and/or discuss each part. The first part can be represented as

$$C_{erg_1}^{g*} = \Upsilon_3\int_0^\infty \frac{e^{-\frac{z}{\delta}}}{(1+z)(\eta+z)^{nL_D}}dz \tag{56}$$

where $C_{erg_1}^{g*}$ represents the first part of the second-hop opportunistic ergodic capacity integral formula. Since it is quite difficult to solve the given integral, we aim to represent it in a simpler form so that we can manipulate and solve it. With the help of partial-fraction decomposition, we can represent the given integral as follows:

$$C_{erg_1}^{g*} = \Upsilon_3\int_0^\infty \left[\overbrace{\sum_{r_3=1}^{nL_D}\frac{\omega_{g1_{r_3}}e^{-\frac{z}{\delta}}}{(\eta+z)^{r_3}}}^{C_{erg_{11}}^{g*}} + \overbrace{\frac{\omega_{g2}e^{-\frac{z}{\delta}}}{(1+z)}}^{C_{erg_{12}}^{g*}}\right]dz \tag{57}$$

where $\omega_{g1_{r_3}}$ and ω_{g2} are obtained using the formulas given in (25a) and (25b), respectively. For part $C_{erg_{11}}^{g*}$ in (57), we exchange the variable in the integral so that $t = 1 + (z/\eta)$; therefore, after some straightforward mathematical manipulations, we get the following:

$$C_{erg_{11}}^{g*} = \Upsilon_3\sum_{r_3=1}^{nL_D}\omega_{g1_{r_3}}\eta^{1-r_3}e^{\frac{\eta}{\delta}}\int_1^\infty \frac{e^{-\frac{\eta}{\delta}t}}{t^{r_3}}dt. \tag{58}$$

Now, by comparing our integral formula with [42, eq. (8.19.3)], we get our desired representation, i.e.,

$$C_{erg_{11}}^{g*} = \Upsilon_3\sum_{r_3=1}^{nL_D}\omega_{g1_{r_3}}\eta^{1-r_3}e^{\frac{\eta}{\delta}}E_{r_3}\left(\frac{\eta}{\delta}\right). \tag{59}$$

For part $C_{erg_{12}}^{g*}$ in (57), we exchange the variable in the integral so that $t = 1 + z$. As a result, we get the following:

$$C_{erg_{12}}^{g*} = \Upsilon_3\omega_{g2}e^{\frac{1}{\delta}}\int_1^\infty \frac{e^{-\frac{z}{\delta}}}{t}dt. \tag{60}$$

With the help of [42, eq. (8.19.3)], we obtain a desired formula, i.e.,

$$C_{erg_{12}}^{g*} = \Upsilon_3\omega_{g2}e^{\frac{1}{\delta}}E_1\left(\frac{1}{\delta}\right). \tag{61}$$

The second part of the second-hop opportunistic ergodic capacity integral formula can be represented as

$$C_{erg_2}^{g*} = \Upsilon_4\int_0^\infty \frac{e^{-\frac{z}{\delta}}}{(\eta+z)^{nL_D-1}(\Lambda_1+z)(\Lambda_2+z)}dz \tag{62}$$

where $C_{erg_2}^{g*}$ represents the second part of the second-hop opportunistic ergodic capacity integral formula. Similar to the first part of the integral, we employ the partial-fraction decomposition technique to represent the given integral in a simpler form so that we can do further mathematical manipulations on it. Thus

$$C_{erg_2}^{g*} = \Upsilon_4\int_0^\infty \left[\overbrace{\sum_{r_4=1}^{nL_D-1}\frac{\omega_{g3_{r_4}}\,e^{-\frac{z}{\delta}}}{(\eta+z)^{r_4}}}^{C_{erg_{21}}^{g*}} + \overbrace{\frac{\omega_{g4}\,e^{-\frac{z}{\delta}}}{(1+z)}}^{C_{erg_{22}}^{g*}} + \underbrace{\frac{\omega_{g5}\,e^{-\frac{z}{\delta}}}{(\Lambda_1+z)}}_{C_{erg_{23}}^{g*}} + \underbrace{\frac{\omega_{g6}\,e^{-\frac{z}{\delta}}}{(\Lambda_2+z)}}_{C_{erg_{24}}^{g*}}\right]dz \tag{63}$$

where $\omega_{g3_{r_4}}$, ω_{g4}, ω_{g5}, and ω_{g6} are obtained using the formulas given in (25c)–(25f), respectively. It can be observed that we obtained similar integral forms as in the first part. Therefore, we just write the final equations as

$$C_{erg_{21}}^{g*} = \Upsilon_4\sum_{r_4=1}^{nL_D-1}\omega_{g3_{r_4}}\eta^{1-r_4}e^{\frac{\eta}{\delta}}E_{r_4}\left(\frac{\eta}{\delta}\right) \tag{64}$$

$$C_{erg_{22}}^{g*} = \Upsilon_4\omega_{g4}e^{\frac{1}{\delta}}E_1\left(\frac{1}{\delta}\right) \tag{65}$$

$$C_{erg_{23}}^{g*} = \Upsilon_4\omega_{g5}e^{\frac{\Lambda_1}{\delta}}E_1\left(\frac{\Lambda_1}{\delta}\right) \tag{66}$$

$$C_{erg_{24}}^{g*} = \Upsilon_4\omega_{g6}e^{\frac{\Lambda_2}{\delta}}E_1\left(\frac{\Lambda_2}{\delta}\right). \tag{67}$$

Finally, the opportunistic ergodic capacity for the second hop can be formulated by combining all derived parts, and it can be written as in (24).

References

[1] S. Haykin, "Cognitive radio: Brain-empowered wireless communications," *IEEE J. Sel. Areas Commun.*, vol. 23, no. 2, pp. 201–220, Feb. 2005.

[2] A. Goldsmith, S. A. Jafar, I. Maric, and S. Srinivasa, "Breaking spectrum gridlock with cognitive radios: An information theoretic perspective," *Proc. IEEE*, vol. 97, no. 5, pp. 894–914, May 2009.

[3] T. Yucek and H. Arslan, "A survey of spectrum sensing algorithms for cognitive radio applications," *IEEE Commun. Surveys Tuts.*, vol. 11, no. 1, pp. 116–130, 1st Quart. 2009.

[4] S. Srinivasa and S. Jafar, "Cognitive radios for dynamic spectrum access—The throughput potential of cognitive radio: A theoretical perspective," *IEEE Commun. Mag.*, vol. 45, no. 5, pp. 73–79, May 2007.

[5] H. Leftah and S. Boussakta, "Novel OFDM based on C-transform for improving multipath transmission," *IEEE Trans. Signal Process.*, vol. 62, no. 23, pp. 6158–6170, Dec. 2014.

[6] J. N. Laneman, D. N. Tse, and G. W. Wornell, "Cooperative diversity in wireless networks: Efficient protocols and outage behavior," *IEEE Trans. Inf. Theory*, vol. 50, no. 12, pp. 3062–3080, Dec. 2004.

[7] A. Forghani, S. Ikki, and S. Aïssa, "On the performance and power optimization of multihop multibranch relaying networks with cochannel interferers," *IEEE Trans. Veh. Technol.*, vol. 62, no. 7, pp. 3437–3443, Sep. 2013.

[8] A. Tukmanov, S. Boussakta, Z. Ding, and A. Jamalipour, "Outage performance analysis of imperfect-CSI-based selection cooperation in random networks," *IEEE Trans. Commun.*, vol. 62, no. 8, pp. 2747–2757, Aug. 2014.

[9] J. Hussein, S. Ikki, S. Boussakta, and C. Tsimenidis, "Performance analysis of the opportunistic multi-relay network with co-channel interference," in *Proc. 22nd EUSIPCO*, Sep. 2014, pp. 166–170.

[10] N. Yang, M. Elkashlan, and J. Yuan, "Impact of opportunistic scheduling on cooperative dual-hop relay networks," *IEEE Trans. Commun.*, vol. 59, no. 3, pp. 689–694, Mar. 2011.

[11] J. Kim, J. Lee, K. Son, S. Song, and S. Chong, "Two-hop opportunistic scheduling in cooperative cellular networks," *IEEE Trans. Veh. Technol.*, vol. 61, no. 9, pp. 4194–4199, Nov. 2012.

[12] K. Hemachandra and N. Beaulieu, "Outage analysis of opportunistic scheduling in dual-hop multiuser relay networks in the presence of interference," *IEEE Trans. Commun.*, vol. 61, no. 5, pp. 1786–1796, May 2013.

[13] H. Zhang, X. Wang, T. Gulliver, W. Shi, and H. Zhang, "Outage performance of MIMO cognitive relay networks with antenna selection," in *Proc. IEEE PACRIM*, Aug. 2013, pp. 10–14.

[14] T. Q. Duong, K. J. Kim, H.-J. Zepernick, and C. Tellambura, "Opportunistic relaying for cognitive network with multiple primary users over Nakagami-*m* fading," in *Proc. IEEE ICC*, Jun. 2013, pp. 5668–5673.

[15] S. Ikki and M. Ahmed, "Performance analysis of cooperative diversity with incremental-best-relay technique over Rayleigh fading channels," *IEEE Trans. Commun.*, vol. 59, no. 8, pp. 2152–2161, Aug. 2011.

[16] H. Chamkhia and M. Hasna, "Performance analysis of relay selection schemes in underlay cognitive networks with imperfect channel state information," in *Proc. ICTC*, Oct. 2013, pp. 556–560.

[17] D. B. da Costa, M. Elkashlan, P. L. Yeoh, N. Yang, and M. Yacoub, "Dual-hop cooperative spectrum sharing systems with multi-primary users and multi-secondary destinations over Nakagami-*m* fading," in *Proc. IEEE 23rd Int. Symp. PIMRC)*, Sep. 2012, pp. 1577–1581.

[18] Y. Huang *et al.*, "Performance analysis of multiuser multiple antenna relaying networks with co-channel interference and feedback delay," *IEEE Trans. Commun.*, vol. 62, no. 1, pp. 59–73, Jan. 2014.

[19] D. Li, "Performance analysis of uplink cognitive cellular networks with opportunistic scheduling," *IEEE Commun. Lett.*, vol. 14, no. 9, pp. 827–829, Sep. 2010.

[20] D. Li, "Performance analysis of MRC diversity for cognitive radio systems," *IEEE Trans. Veh. Technol.*, vol. 61, no. 2, pp. 849–853, Feb. 2012.

[21] T. Q. Duong, D. Benevides da Costa, M. Elkashlan, and V. N. Q. Bao, "Cognitive amplify-and-forward relay networks over Nakagami-*m* fading," *IEEE Trans. Veh. Technol.*, vol. 61, no. 5, pp. 2368–2374, Jun. 2012.

[22] T.-T. Tran, V. N. Q. Bao, V. D. Thanh, and T.-D. Nguyen, "Performance analysis of spectrum sharing-based multi-hop decode-and-forward relay networks under interference constraints," in *Proc. ICCE)*, Aug. 2012, pp. 200–205.

[23] T. Q. Duong, P. L. Yeoh, V. N. Q. Bao, M. Elkashlan, and N. Yang, "Cognitive relay networks with multiple primary transceivers under spectrum-sharing," *IEEE Signal Process. Lett.*, vol. 19, no. 11, pp. 741–744, Nov. 2012.

[24] Y. Huang *et al.*, "Outage analysis of spectrum sharing relay systems with multiple secondary destinations under primary user's interference," *IEEE Trans. Veh. Technol.*, vol. 63, no. 7, pp. 3456–3464, Sep. 2014.

[25] V. N. Q. Bao, T. Q. Duong, D. Benevides da Costa, G. Alexandropoulos, and A. Nallanathan, "Cognitive amplify-and-forward relaying with best relay selection in non-identical Rayleigh fading," *IEEE Commun. Lett.*, vol. 17, no. 3, pp. 475–478, Mar. 2013.

[26] F. Khan, K. Tourki, M.-S. Alouini, and K. Qaraqe, "Outage and SER performance of spectrum sharing system with TAS/MRC," in *Proc. IEEE ICC Workshops*, Jun. 2013, pp. 381–385.

[27] S. Mishra and A. Trivedi, "Exploiting opportunistic decode-and-forward cooperation for cognitive radio relay channels in multi-antenna cognitive radio networks," in *Proc. Int. Conf. Adv. Comput., Commun. Inf.*, Aug. 2013, pp. 155–158.

[28] Y. Huang *et al.*, "Cognitive MIMO relaying networks with primary user's interference and outdated channel state information," *IEEE Trans. Commun.*, vol. 62, no. 12, pp. 4241–4254, Dec. 2014.

[29] A. Hyadi, M. Benjillali, M.-S. Alouini, and D. B. da Costa, "Performance analysis of underlay cognitive multihop regenerative relaying systems with multiple primary receivers," *IEEE Trans. Wireless Commun.*, vol. 12, no. 12, pp. 6418–6429, Dec. 2013.

[30] F. Guimaraes, D. B. da Costa, T. Tsiftsis, C. Cavalcante, and G. Karagiannidis, "Multiuser and multirelay cognitive radio networks under spectrum-sharing constraints," *IEEE Trans. Veh. Technol.*, vol. 63, no. 1, pp. 433–439, Jan. 2014.

[31] X. Jia, L. Yang, and H. Zhu, "Cognitive opportunistic relaying systems with mobile nodes: Average outage rates and outage durations," *IET Commun.*, vol. 8, no. 6, pp. 789–799, Apr. 2014.

[32] D. Li, "Cognitive relay networks: Opportunistic or uncoded decode-and-forward relaying?" *IEEE Trans. Veh. Technol.*, vol. 63, no. 3, pp. 1486–1491, Mar. 2014.

[33] L. Fan, X. Lei, T. Q. Duong, R. Q. Hu, and M. Elkashlan, "Multiuser cognitive relay networks: Joint impact of direct and relay communications," *IEEE Trans. Wireless Commun.*, vol. 13, no. 9, pp. 5043–5055, Sep. 2014.

[34] J. Hussein, S. Ikki, S. Boussakta, and C. Tsimenidis, "Performance study of the dual-hop underlay cognitive network in the presence of co-channel interference," in *Proc. IEEE 81st VTC Spring*, May 2015, pp. 1–5.

[35] X. Kang, Y.-C. Liang, and A. Nallanathan, "Optimal power allocation for fading channels in cognitive radio networks: Delay-limited capacity and outage capacity," in *Proc. IEEE Veh. Technol. Conf. Spring*, May 2008, pp. 1544–1548.

[36] H. Yu, I.-H. Lee, and G. Stüber, "Outage probability of decode-and-forward cooperative relaying systems with co-channel interference," *IEEE Trans. Wireless Commun.*, vol. 11, no. 1, pp. 266–274, Jan. 2012.

[37] S. Ikki, P. Ubaidulla, and S. Aïssa, "Performance study and optimization of cooperative diversity networks with co-channel interference," *IEEE Trans. Wireless Commun.*, vol. 13, no. 1, pp. 14–23, Jan. 2014.

[38] M. Hasna and M.-S. Alouini, "Outage probability of multihop transmission over Nakagami fading channels," *IEEE Commun. Lett.*, vol. 7, no. 5, pp. 216–218, May 2003.

[39] S. Ikki and S. Aïssa, "Performance analysis of dual-hop relaying systems in the presence of co-channel interference," in *Proc. IEEE GLOBECOM*, Dec. 2010, pp. 1–5.

[40] M. Hasna and M.-S. Alouini, "End-to-end performance of transmission systems with relays over Rayleigh-fading channels," *IEEE Trans. Wireless Commun.*, vol. 2, no. 6, pp. 1126–1131, Nov. 2003.

[41] M. Abramowitz and I. A. Stegun, *Handbook of Mathematical Functions: With Formulas, Graphs, and Mathematical Tables*. New York, NY, USA: Dover, 1972.

[42] F. W. J. Olver, D. W. Lozier, R. F. Boisvert, and C. W. Clark, Eds., *NIST Handbook of Mathematical Functions*. New York, NY, USA: Cambridge Univ. Press, 2010.

[43] Z. Wang and G. Giannakis, "A simple and general parameterization quantifying performance in fading channels," *IEEE Trans. Commun.*, vol. 51, no. 8, pp. 1389–1398, Aug. 2003.

Jamal Ahmed Hussein (S'04) received the B.Sc. degree (first-class honors) in electrical engineering from the Electrical Department, College of Engineering, University of Salahaddin, Erbil, Iraq, in 2001 and the M.Sc. degree in electrical engineering from the Electrical Department, College of Engineering, University of Sulaimani, Sulaimani, Iraq, in 2007. He is currently working toward the Ph.D. degree in communication and signal processing with the School of Electrical and Electronic Engineering, Newcastle University, Newcastle Upon Tyne, U.K.

His research interests include wireless communication, cooperative communication, cognitive radio, and energy harvesting.

Salama S. Ikki (M'15) received the B.S. degree from Al-Isra University, Amman, Jordan, in 1996; the M.Sc. degree from The Arab Academy for Science and Technology and Maritime Transport, Alexandria, Egypt, in 2002; and the Ph.D. degree from Memorial University, St. Johns, NL, Canada, in 2009, all in electrical engineering.

From February 2009 to February 2010, he was a Postdoctoral Researcher with the University of Waterloo, Waterloo, ON, Canada. From February 2010 to December 2012, he was a Research Assistant with the Institut National de la Recherche Scientifique, University of Quebec, Montreal, QC, Canada. He is currently an Assistant Professor of wireless communications with Lakehead University, Thunder Bay, ON. He is the author of 100 journal and conference papers and has more than 2000 citations and an H-index of 23. His research interests include cooperative networks, multiple-input multiple-output, spatial modulation, and wireless sensor networks.

Dr. Ikki has served as a Technical Program Committee Member for various conferences, including the IEEE International Conference on Communications; the IEEE Global Communications Conference; the IEEE Wireless Communications and Networking Conference; the IEEE Spring/Fall Vehicular Technology Conference; and the IEEE International Symposium on Personal, Indoor, and Mobile Communications. He currently serves on the Editorial Board of the IEEE COMMUNICATIONS LETTERS and the *Institution of Engineering and Technology Communications.* He received a Best Paper Award for his paper published in the EURASIP *Journal on Advanced Signal Processing*. He also received IEEE COMMUNICATIONS LETTERS, IEEE WIRELESS COMMUNICATIONS LETTERS, and IEEE TRANSACTIONS ON VEHICULAR TECHNOLOGY Exemplary Reviewer Certificates for 2012, 2012, and 2014, respectively.

Said Boussakta (S'89–M'90–SM'04) received the "Ingenieur d'Etat" degree in electronic engineering from the National Polytechnic Institute of Algiers, Algiers, Algeria, in 1985 and the Ph.D. degree in electrical engineering from Newcastle University, Newcastle Upon Tyne, U.K., in 1990.

During 1990–1996, he was with Newcastle University as a Senior Research Associate in digital signal processing. During 1996–2000, he was a Senior Lecturer in communication engineering with Teesside University, Middlesbrough, U.K. During 2000–2006, he was a Reader in digital communications and signal processing with the University of Leeds, Leeds, U.K. He is currently a Professor of communications and signal processing with the School of Electrical and Electronic Engineering, Newcastle University, where he lectures on communication networks and signal processing. He has authored and coauthored more than 200 publications. His research interests include fast digital signal processing algorithms, digital communications, communication network systems, cryptography, and digital signal/image processing.

Dr. Boussakta served as the Chair for the Signal Processing for Communications Symposium at the 2006, 2007, 2008, 2010, and 2013 IEEE International Conference on Communications. He is a Fellow of the Institution of Engineering and Technology and a Senior Member of the Communications and Signal Processing Societies.

Charalampos C. Tsimenidis (M'05–SM'12) received the M.Sc. (with distinction) and Ph.D. degrees in communications and signal processing from Newcastle University, Newcastle Upon Tyne, U.K., in 1999 and 2002, respectively.

He is a Senior Lecturer in signal processing for communications with the School of Electrical and Electronic Engineering, Newcastle University. During the last 12 years, he has published over 180 conference and journal papers, successfully supervised three M.Phil. and 28 Ph.D. students, and made contributions in the area of receiver design to several European-funded research projects, including Long Range Telemetry in Ultra-Shallow Channels (LOTUS), Shallow Water Acoustic Network (SWAN), and Acoustic Communication Network for the Monitoring of the Underwater Environment in Coastal Areas (ACME). His main research interests include adaptive array receivers for wireless communications, including demodulation algorithms and protocol design for underwater acoustic channels.